Thin layering in tailings deposits and its implications for CPT-based state parameter estimation

Abideen T. Owolabi[1] and Luis A. Torres-Cruz[2*]

[1]School of Civil and Environmental Engineering, University of the Witwatersrand, Johannesburg, South Africa.

[2]Assistant Professor, Norman B. Keevil Institute of Mining Engineering, University of British Columbia, Vancouver, Canada. Email: Luis.TorresCruz@ubc.ca

[*]Corresponding author. Email: Luis.TorresCruz@ubc.ca

Total word count: 3238

ABSTRACT

The cone penetration test (CPT) is used to characterize tailings and infer the state parameter (ψ) using methods calibrated on uniform specimens. This work explores whether subaerially deposited tailings resemble uniform specimens. We quantified layering in tube samples from three active gold tailings storage facilities and visually appraised a 3 m profile at a fourth. Pronounced thin layering was found in every sample and in the exposed profile; the thickest apparently uniform layer was ~15 cm, far below the >0.6 m thickness recommended for ψ estimates. The variability of particle size distribution within a single 25 cm sample frequently matched or exceeded that measured across two entire impoundments of different commodities. At the observed layer thicknesses the cone cannot develop an isolated-layer response, so several layers jointly govern its readings. Thin layering is therefore a clear departure from the uniformity assumption underpinning widely used CPT interpretation methods, and it also obstructs the very testing that would be needed to characterize the resulting error. We conclude that, for subaerially deposited tailings, the confidence currently placed in CPT-based ψ estimates exceeds what the evidence supports. We argue for more space for the characterization of specimens that preserve in situ layering.

Keywords: cone penetration testing, tailings, layering, state parameter, stratified deposit

1 INTRODUCTION

The cone penetration test (CPT) is the most widely used in situ test for characterizing tailings. Several interpretation methods infer the state parameter (ψ), which is the difference between void ratio and critical state line (CSL) at the current mean effective stress, because ψ is a useful predictor of mechanical behavior (Been & Jefferies 1985). The earliest such methods were built from calibration chamber (CC) tests supplemented by triaxial testing (Been et al. 1986, 1987a), an approach referred to hereafter as the Been et al. framework. Both the CC and triaxial specimens were deliberately uniform: a single void ratio and a constant particle size distribution (PSD), particle shape, and mineralogy, so that a unique ψ could be defined and correlated with cone tip resistance (e.g., Been et al. 1987b).

Subsequent work expanded the framework, including cavity-expansion simulations that remove the need for site-specific CC tests (Shuttle & Jefferies 1998). The newer methods, however, remain calibrated against CC results and continue to rely on properties defined for uniform soils (e.g., Plewes et al. 1992; Shuttle & Cunning 2007; Shuttle & Jefferies 2016; Jefferies et al. 2019; Shuttle et al. 2022; Jung et al. 2025). This framework features prominently in the investigations of major tailings storage facility (TSF) failures, including Samarco, Cadia Valley, and Brumadinho (Morgenstern et al. 2016; Jefferies et al. 2019; Robertson et al. 2019; CIMNE 2021).

This prominence prompts the question of how closely tailings deposits resemble the uniform specimens that underpin the Been et al. framework. Layered deposits complicate CPT interpretation in two ways: they depart from the conditions under which the framework was developed, and they cause several soils to influence the cone simultaneously (Ahmadi & Robertson 2005). It is then unclear which of the layered soils should be selected for laboratory testing, and the use of homogenized samples for interpretation in layered ground has, to our knowledge, never been validated. To avoid interference from adjacent layers it has been recommended that interpretation focus on layers thicker than 0.6 m (Jefferies & Been 2016).

Layering in tailings has often been reported incidentally or qualitatively (Høeg et al. 2000; Jacobsz & Narainsamy 2022). Quantitative characterizations are scarce and inconsistent: some report deposits stratified into layers only centimetres thick (Vermeulen 2001; Reid et al. 2018c, 2022), with one noting the resulting challenge to critical state soil mechanics (Reid et al. 2018c), while others find only modest layering (Reid et al. 2018a; Reid & Fanni 2022). The prevalence of layering therefore remains unclear. This issue warrants attention given the consequences of TSF failures and the current absence of experimental validation of CPT-based ψ in tailings (Fourie et al. 2022). Accordingly, we characterized the layering in high-quality samples from three active South African gold TSFs using contrasting deposition methods, and visually appraised a 3 m profile at a fourth. The results are discussed in the context of CPT-based ψ inference, and supplementary characterization approaches are suggested.

2 METHODOLOGY

Methodological details not central to the argument are given in the supplementary file.

2.1 Sites investigated

Fieldwork focused on four upstream gold TSFs near Johannesburg, South Africa (Figs S1, S2). High-quality surficial samples that preserved in situ layering were taken from three active TSFs chosen to represent distinct deposition methods; cycloning, paddocking, and spigotting (McPhail & Wagner 1987), and referred to as the Cyclone, Paddock, and Spigot TSFs. The fourth TSF, under reclamation, allowed a 3 m profile to be exposed and is referred to as the Remine TSF.

2.2 Sampling and characterization

A stainless steel split-tube sampler compliant with ASTM D1587-15 (Fig S3) was used to extract surficial samples 25 cm long. Each sample was cut into 25 slices, 1 cm thick, numbered 1 to 25 from top to bottom (Fig S4). Ten samples, 250 slices in total, were collected at subaerially deposited locations (Table 1): the underflow and overflow at the Cyclone TSF, and a range of distances from the discharge point at the Paddock and Spigot TSFs. For every slice the PSD was measured by laser diffraction and the plastic limit (PL) by thread rolling. All sampled tailings were angular (Fig S5) and quartz-dominated (Table S1).

Table 1. Location and code of the ten samples recovered with the tube sampler.

TSF	Location	Code
Cyclone	9 m along outer wall from underflow discharge (Figure S2a).	Cyclone UnFl
	35 m towards the decant pond from overflow discharge (Figure S2a).	Cyclone OvFl
Paddock	25, 50, 75, and 100 m from discharge within the paddock (Figure S2b).	Paddock @25, Paddock @50, Paddock @75, Paddock @100
Spigot	25, 50, 75, and 100 m from discharge towards the decant pond (Figure S2c).	Spigot @25, Spigot @50, Spigot @75, Spigot @100

2.3 Profiling at the Remine TSF

Reclamation at the Remine TSF allowed a 3 m deep profile to be exposed as six 0.5 m benches cut with a spade (Fig S2d). Each vertical face was photographed for visual appraisal of layering.

3 RESULTS

3.1 Layering in the sampled tailings

All ten samples spanned a range of PSDs (Figs S6–S8). The corresponding profiles of D_{10}, D_{50}, and D_{90} (Fig 1) show that gradation changes over distances of a few centimetres. The thickest apparently uniform interval in any sample was the upper ~15 cm of the Cyclone overflow sample (Fig 1b).

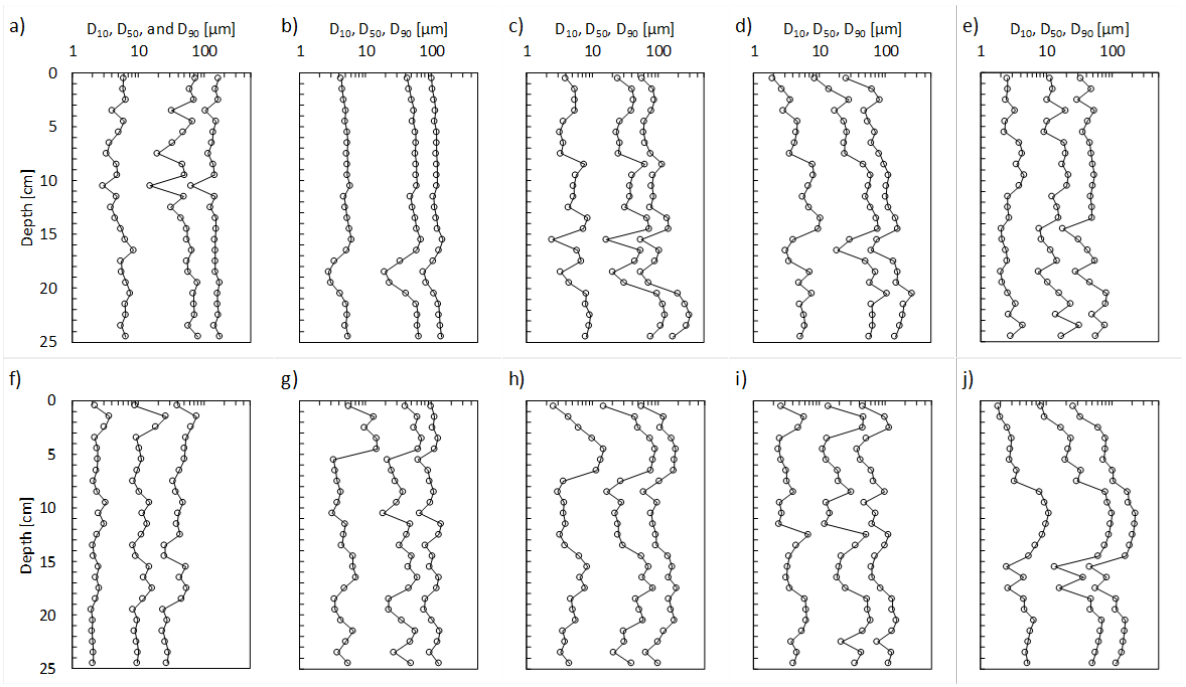

84

85 **Fig. 1.** *Profiles of D_{10}, D_{50}, and D_{90} of samples a) Cyclone UnFl, b) Cyclone OvFl, c) Paddock @25, d) Paddock @50,*

86 *e) Paddock @75, f) Paddock @100, g) Spigot @25, h) Spigot @50, i) Spigot @75, and j) Spigot @100.*

87 To contextualise the PSD variability, Fig 2 compares the spread of D_{50} within each 25 cm sample against

88 the D_{50} spread in subaerially deposited samples across two entire TSFs: the platinum tailings at Impala (49

89 PSDs; Torres Cruz 2019) and the iron tailings at Brumadinho (33 PSDs from two campaigns; Pirete da

90 Silva 2010 and Robertson et al. 2019). Spread is expressed as the ratio of the 90th to 10th percentile

91 (P90/P10) of D_{50}, a measure that, by excluding the lowest and highest 10%, reduces dependence on the

92 number of samples favoring a fair comparison between differently-sized populations (i.e. 25, 49, and 33).

93 The within-sample spread of 8 of the 10 samples equalled or exceeded the whole-TSF spread of Impala and

94 Brumadinho (2.3–2.5×). TSF comparators were measured by sieve and hydrometer whereas the slices were

95 measured by laser diffraction. While these methods rely on different physical mechanisms, the comparison

96 remains highly informative of broad distributional trends.

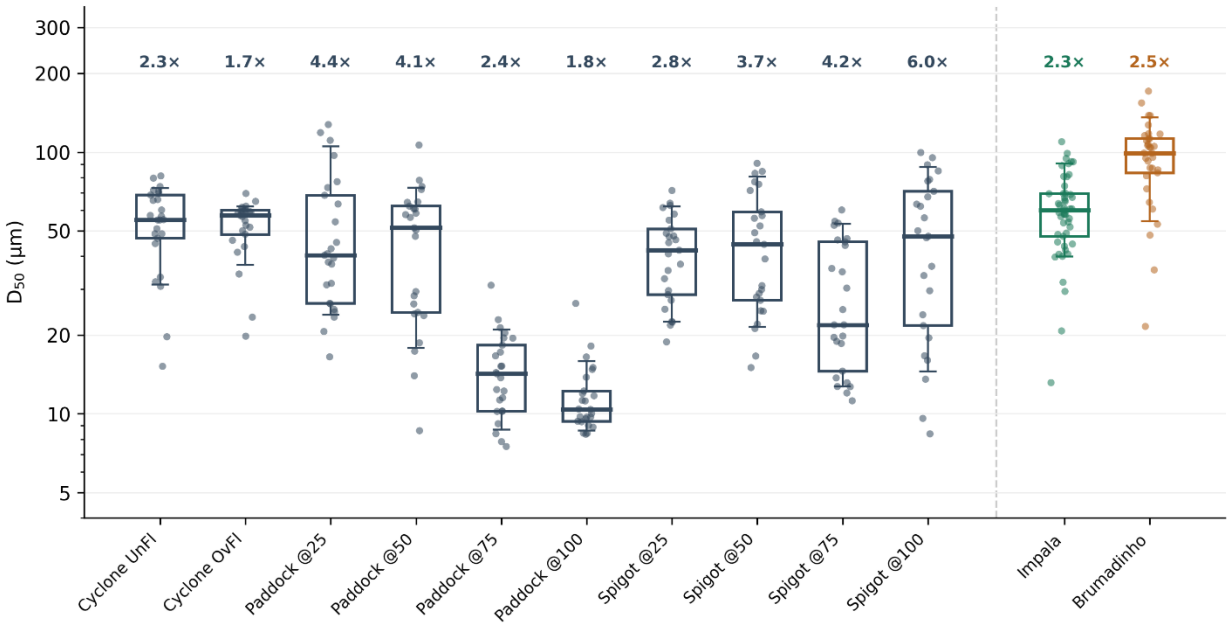

Fig. 2. *Within-sample versus whole-deposit spread of* D_{50}. *Each gold-tailings sample and each whole-deposit comparator is shown as a dot strip with a box (Q25–Q75), median line, and whiskers at P10–P90. The annotated factor is the spread P90/P10. Sample data are laser diffraction; comparators are sieve/hydrometer.*

Plastic limits, where measurable, fell within a narrow band of 23–33%, but most slices were non-plastic (Table S2). Thus, while PSD varied markedly within a sample, plasticity did not.

3.2 Layering in the exposed Remine profile

The 3 m Remine profile (Fig 3) was thinly layered, on the assumption that colour changes track changes in PSD or mineralogy. Several intervals showed layers only a few millimetres thick, and no layer appeared to exceed about 10 cm.

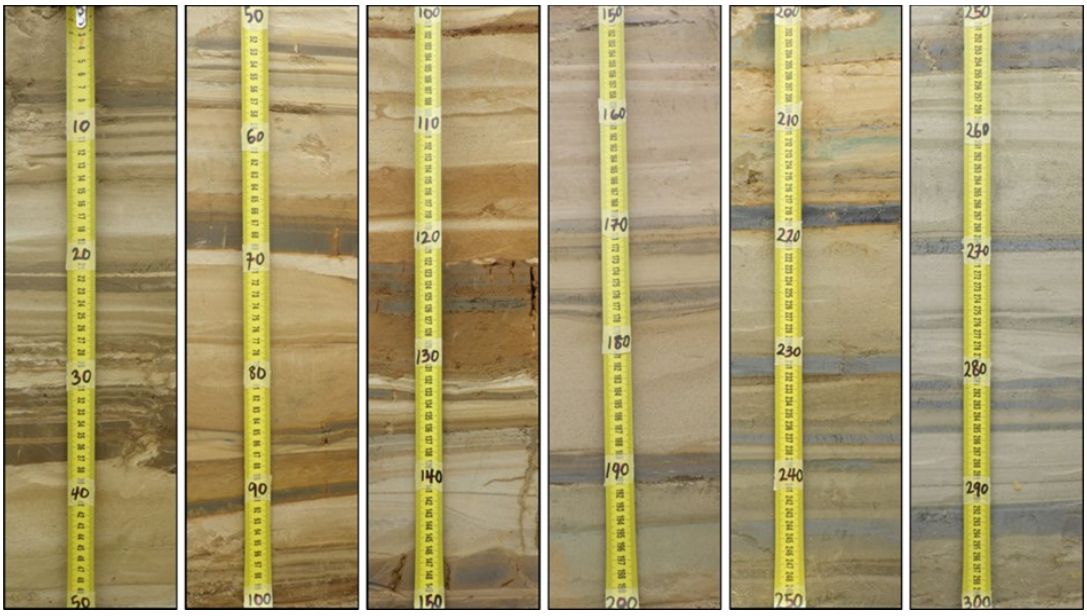

Fig. 3. *The 3 m deep profile exposed at the Remine TSF. The measuring tape is graduated in centimetres.*

4 DISCUSSION

The thickest apparently uniform layer, ~15 cm, documented here is already well below the >0.6 m thickness recommended for ψ inference (Jefferies & Been 2016). Expressed as a normalized thickness, ~15 cm corresponds to $H/d \approx 4$ for a standard 35.7 mm (10 cm²) cone. Cone tip resistance is influenced over a zone of roughly 10–30 cone diameters (Ahmadi & Robertson 2005), depending on soil stiffness. Even taking the lower bound of that range and the thickest uniform layer observed, the layer is too thin for the cone to develop an isolated-layer response. Figs 1 and 3 suggest that such thin layering is the norm in subaerially deposited tailings. Fig 2 highlights that significance of the PSD variations across layers: they are comparable and often exceed the variations observed between samples of subaerially deposited tailings in entire TSFs.

This has a direct consequence for the standing recommendation to characterize multiple PSDs within a TSF (Jefferies & Been 2016). That recommendation is consistent with the variety of PSDs in a TSF, but it does not address the fact that these PSDs do not exist as thick, separately interpretable layers. They exist as thin strata that respond to the cone jointly. The difficulty is compounded if, as is plausible although not explored

herein, ψ itself varies between layers. This would constitute a further departure from the framework's assumptions.

Thin layering does more than introduce error into ψ estimates: it obstructs the testing that would be needed to characterize that error. Validating any CPT-based method requires direct comparison against ψ measured on high-quality specimens. But ψ is defined as the distance of a soil's void ratio from its CSL, and where PSD changes from layer to layer, so does the CSL (Torres-Cruz 2019). A layered validation specimen therefore has no single CSL. A void ratio recorded for the entire specimen describes a composite value rather than the state of one. Layering thus simultaneously undermines the estimate and its potential validation.

These observations bear on the method most highly regarded in tailings practice. The widget method (Shuttle & Cunning 2007; Shuttle & Jefferies 2016; Jefferies et al. 2019; Shuttle et al. 2022) was judged the most reliable of four CPT-based ψ methods by the Brumadinho expert panel and was adopted in subsequent Brumadinho and Cadia investigations (Robertson et al. 2019; CIMNE 2021; Jefferies et al. 2019). Yet a comparison across three TSFs found that ψ from the widget method and ψ from "undisturbed" samples did not, overall, agree (Fourie et al. 2022). Thin layering is a plausible contributor to that disagreement, alongside other documented limitations of the framework: its calibration on predominantly dilatant CC sands, its reliance on seldom-measured in situ horizontal stress, partial drainage during penetration, and the conversion of pore pressure between measurement and modelling positions (Ayala et al. 2022; Fourie et al. 2022; Ayala et al. 2023; Jefferies et al. 2019). Taken together, these suggest that, for subaerially deposited tailings, the confidence currently placed in CPT-based ψ exceeds what the evidence supports.

This has practical implications. Recent ICOLD (2025) guidance notes that high-quality specimens, though the most direct route to in situ void ratio, may be "extremely costly," "impossible," or "unreliable", and positions the CPTu with ψ correlations from Jefferies and Been (2016) as the most practical option. This

147 weighting in favor of CPT-based ψ to the detriment of high-quality sampling seems unwarranted in light of
148 the results and discussion herein.

149 Regarding alternative characterization approaches, there are two alternatives we believe should be carefully
150 considered. First, the more empirical CPT interpretation methods derived from back-analysis of failure case
151 histories (e.g., Olson & Stark 2002; Robertson 2022) sit more comfortably with our limited ability to
152 characterize layered deposits, even acknowledging their own shortcomings (Fourie et al. 2022). Second,
153 the profession should make more space for the approximate characterization of high-quality specimens that
154 preserve, at least partially, the in situ layered fabric and density, rather than concentrating effort on the
155 precise characterization of uniform specimens that do not resemble in situ layering. Such testing is
156 necessarily approximate, but the literature shows it can be informative. Undisturbed specimens have
157 revealed dilative behaviour masked by reconstitution (Høeg et al. 2000), enabled estimates of desiccation-
158 induced strength (Reid et al. 2018b, 2018c), and supported parameter estimation in failure investigations
159 (da Fonseca et al. 2020). A 2030 outlook survey of tailings engineers likewise identified better undisturbed
160 sampling as a priority (Small et al. 2024).

161 ## 5 CONCLUSIONS

162 Widely used CPT interpretation methods infer ψ from a framework built on uniform CC and triaxial
163 specimens. We examined whether subaerially deposited gold tailings resemble such specimens. In ten 25
164 cm tube samples from three TSFs and in a 3 m exposed profile at a fourth, thin layering was found
165 throughout. The thickest apparently uniform layer did not exceed ~0.15 m, against a recommended >0.6 m,
166 and within-sample PSD variability often matched or exceeded that of entire impoundments of different
167 commodities.

168 At these thicknesses the cone response integrates several layers, so the deposits depart materially from the
169 uniformity the Been et al. framework assumes. The same layering also obstructs the validation that would
170 be needed to quantify the resulting error. For subaerially deposited tailings, therefore, the confidence placed

in CPT-based ψ estimates exceeds what the evidence supports. We propose that tailings engineering allow more room for the approximate characterization of high-quality specimens that preserve their in situ layering, consistent with the principle that "it is better to be vaguely right than exactly wrong" (Read 1920).

COMPETING INTERESTS

The authors declare there are no competing interests.

DATA AVAILABILITY STATEMENT

Data generated or analyzed during this study are provided in full within the published article and its supplementary materials.

ACKNOWLEDGEMENTS

This Note is based on the doctoral research of the first author, supervised by the second. The authors gratefully acknowledge financial support from Anglo American and logistic support from DRD Gold, Gold Fields, and Sibanye Stillwater.

REFERENCES

Ahmadi, M.M., & Robertson, P.K. (2005). Thin-layer effects on the CPT qc measurement. Canadian Geotechnical Journal, 42(5), 1302–1317.

ASTM. (2015). ASTM D1587M-15 Standard practice for thin-walled tube sampling of fine-grained soils for geotechnical purposes.

Ayala, J., Fourie, A., & Reid, D. (2022). Improved cone penetration test predictions of the state parameter of loose mine tailings. Canadian Geotechnical Journal.

Ayala, J., Fourie, A., & Reid, D. (2023). A Unified Approach for the Analysis of CPT Partial Drainage Effects within a Critical State Soil Mechanics Framework in Mine Tailings. J. Geotech. Geoenviron. Eng., 149(6).

Been, K., & Jefferies, M. (1985). A state parameter for sands. Géotechnique, 35(2), 99–112.

Been, K., Crooks, J., Becker, D., & Jefferies, M. (1986). The cone penetration test in sands: part I, state parameter interpretation. Géotechnique, 36(2), 239–249.

Been, K., Jefferies, M., Crooks, J., & Rothenburg, L. (1987a). The cone penetration test in sands: part II, general inference of state. Géotechnique, 37(3), 285–299.

Been, K., Lingnau, B., Crooks, J., & Leach, B. (1987b). Cone penetration test calibration for Erksak (Beaufort Sea) sand. Canadian Geotechnical Journal, 24(4), 601–610.

CIMNE. (2021). Computational analyses of Dam I failure at the Corrego de Feijao mine in Brumadinho.

da Fonseca, A., Cordeiro, D., Molina-Gómez, F., & Fonseca, A. (2020). Annex 1: New site investigation and experimental campaign [in Portuguese]. In CIMNE, Computational analyses of Dam I failure at the Corrego de Feijao mine in Brumadinho.

Fourie, A., Verdugo, R., Bjelkevik, A., Torres-Cruz, L., & Znidarcic, D. (2022). Geotechnics of mine tailings: a 2022 state of the art. In Proceedings of the 20th ICSMGE (pp. 121–183). Australian Geomechanics Society.

Høeg, K., Dyvik, R., & Sandbækken, G. (2000). Strength of undisturbed versus reconstituted silt and silty sand specimens. Journal of Geotechnical and Geoenvironmental Engineering, 126(7), 606–617.

ICOLD. (2025). Tailings Dam Safety: Bulletin 194. CRC Press/Balkema.

Jacobsz, S., & Narainsamy, Y. (2022). Field and laboratory research into the undrained behaviour of tailings at the University of Pretoria. Journal of the SAIMM, 122(6), 267–273.

Jefferies, M., & Been, K. (2016). Soil Liquefaction — A Critical State Approach, 2nd ed. CRC Press.

Jefferies, M., Morgenstern, N., Van Zyl, D., & Wates, J. (2019). Report on NTSF Embankment Failure. Cadia Valley Operations for Ashurst Australia.

Jung, H., Lin, J., & Stark, T. (2025). Sand state parameter from CPT. Canadian Geotechnical Journal, 62, 1–16.

McPhail, G., & Wagner, J. (1987). Disposal of residues. In The Extractive Metallurgy of Gold in South Africa.

Morgenstern, N., Vick, S., Viotti, C., & Watts, B. (2016). Report on the Immediate Causes of the Failure of the Fundão Dam.

Olson, S.M., & Stark, T.D. (2002). Liquefied strength ratio from liquefaction flow failure case histories. Canadian Geotechnical Journal, 39(3), 629–647.

Pirete da Silva, W. (2010). Study of the static liquefaction potential of an upstream tailings dam applying Olson's (2001) methodology [In Portuguese]. Masters thesis from the Federal University of Ouro Preto, Brazil.

Plewes, H., Davies, M., & Jefferies, M. (1992). CPT based screening procedure for evaluating liquefaction susceptibility. In Proc. 45th Canadian Geotechnical Conference, Toronto.

Read, C. (1920). Logic: Deductive and Inductive. London: Simkin, Marshall.

Reid, D., & Fanni, R. (2022). A comparison of intact and reconstituted samples of a silt tailings. Géotechnique, 72(2), 176–188.

Reid, D., Fanni, R., Koh, K., & Orea, I. (2018a). Characterisation of a subaqueously deposited silt iron ore tailings. Géotechnique Letters, 8(4), 278–283.

Reid, D., Fourie, A., & Russell, A. (2018b). Effects of desiccation on shear strength of tailings. In Proceedings of Tailings and Mine Waste 2018.

Reid, D., Fourie, A., Castro, J., & Lupo, J. (2018c). Undrained shear strength evolution with loading on an undisturbed block sample of desiccated gold tailings. In Proceedings of Tailings and Mine Waste 2018.

Reid, D., Fourie, A., & Fanni, R. (2022). Layering — the missing factor in fabric studies? In Proc. 20th ICSMGE. Australian Geomechanics Society.

Robertson, P.K. (2022). Evaluation of flow liquefaction and liquefied strength using the cone penetration test: an update. Canadian Geotechnical Journal, 59(4), 620-624.

Robertson, P., de Melo, L., Williams, D., & Wilson, G. (2019). Report of the Expert Panel on the Technical Causes of the Failure of Feijão Dam I.

Shuttle, D., & Cunning, J. (2007). Liquefaction potential of silts from CPTu. Canadian Geotechnical Journal, 44(1), 1–19.

Shuttle, D., & Jefferies, M. (1998). Dimensionless and unbiased CPT interpretation in sand. Int. J. for Numerical and Analytical Methods in Geomechanics, 22(5), 351–391.

Shuttle, D., & Jefferies, M. (2016). Determining silt state from CPTu. Geotechnical Research, 3(3), 90–118.

244 Shuttle, D., Marinelli, F., Brasile, S., & Jefferies, M. (2022). Validation of computational liquefaction for tailings: Tar
245 Island slump. Geotechnical Research, 9(1), 32–55.
246 Small, A., Witte, A., & Bjelkevik, A. (2024). What could tailings facility engineering look like in 2030? In Proceedings
247 of Tailings and Mine Waste 2024.
248 Torres-Cruz, L. (2019). Limit void ratios and steady-state line of non-plastic soils. Proceedings of the ICE —
249 Geotechnical Engineering, 172(3), 283–295.
250 Vermeulen, N. (2001). The composition and state of gold tailings. PhD thesis, University of Pretoria.
251

Supplementary Material

Supplementary material

Thin layering in tailings deposits and its implications for CPT-based state parameter estimation

Abideen T. Owolabi and Luis A. Torres-Cruz

This document provides the supplementary figures (Figs S1–S8) and tables (Tables S1 and S2) referenced in the Note. It expands on the site descriptions, sampling and characterization procedures, and presents the particle size distribution (PSD) curves of the individual samples.

S1 Sites investigated

The fieldwork focused on gold tailings from the Witwatersrand Basin near Johannesburg, South Africa (Fig S1). Four upstream tailings storage facilities (TSFs) were investigated. Their locations and the sampling points within them are shown in Figs S1 and S2.

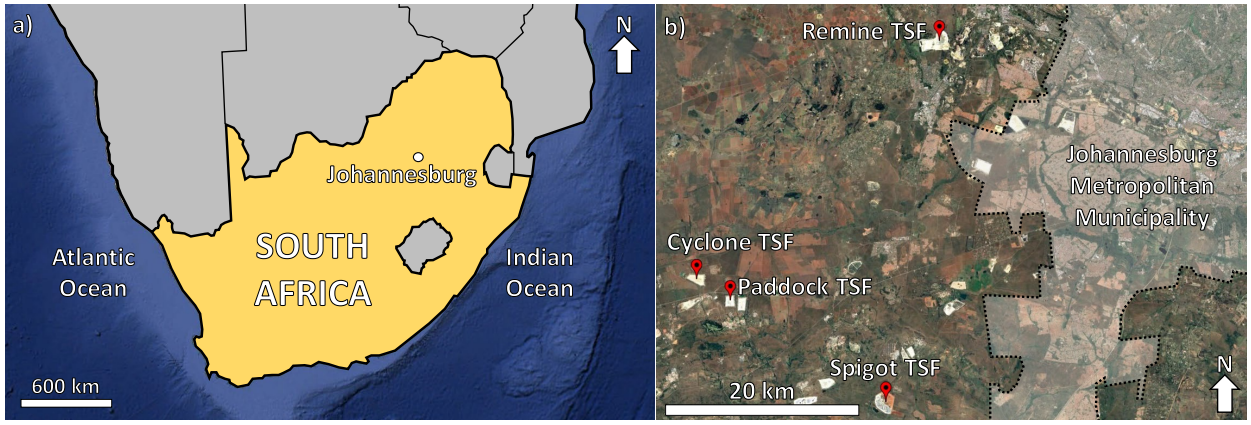

Fig. S1. *Location of the TSFs: a) location of Johannesburg within South Africa; and b) location of the TSFs with respect to Johannesburg. Source: Google Earth Pro.*

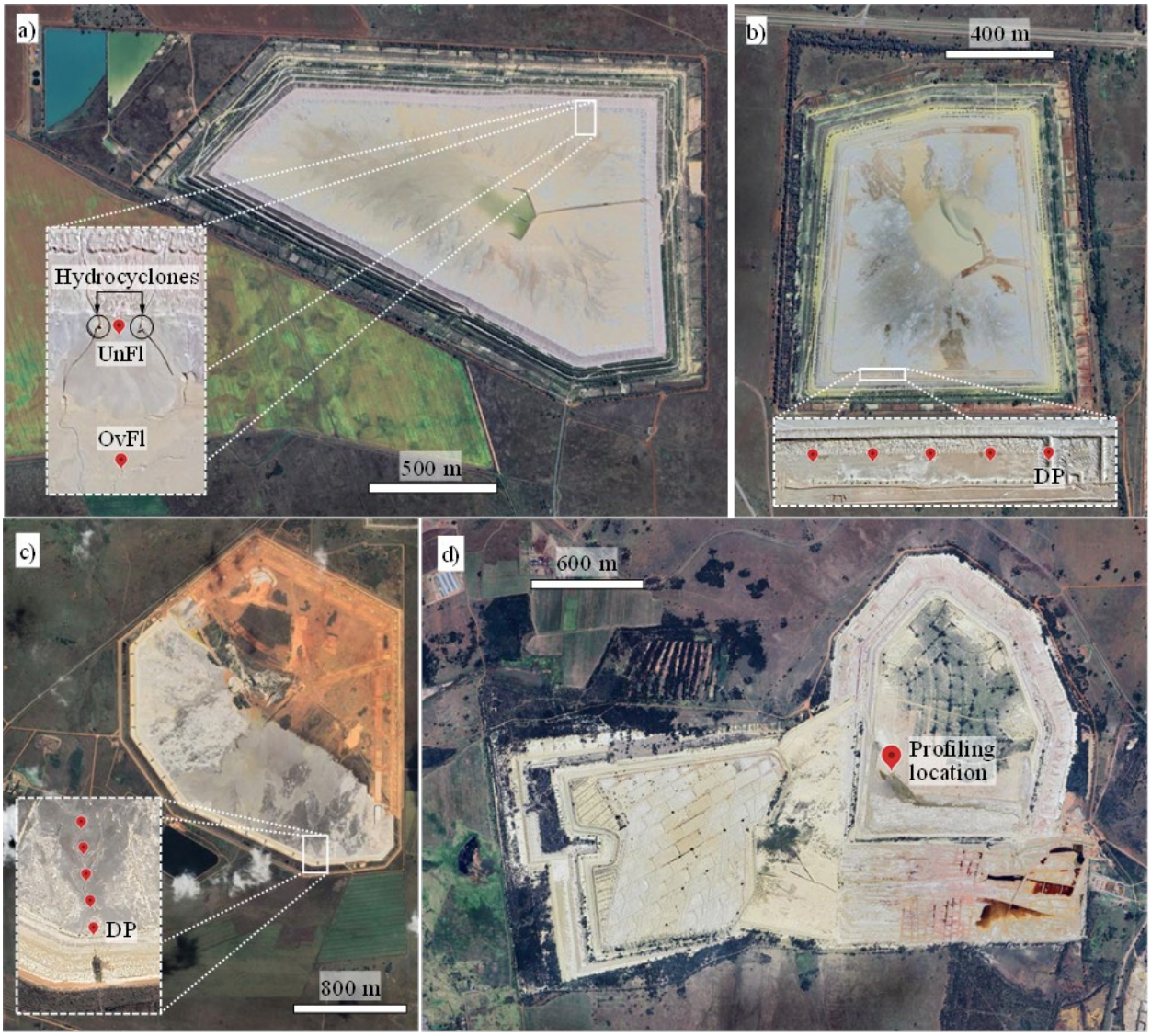

Fig. S2. *Satellite images of the investigated TSFs: a) Cyclone TSF; b) Paddock TSF; c) Spigot TSF; and d) Remine TSF. Insets in parts a) to c) show the sampling locations. OvFl = overflow; UnFl = underflow; DP = discharge point (not sampled). Source: Google Earth Pro.*

S2 Sampling and characterization of tailings

S2.1 Sampler and slicing procedure

A stainless-steel split-tube sampler (Fig S3) was manufactured to extract surficial samples that preserved any potential layering. The sampler meets the requirements of ASTM D1587-15 (ASTM

2015) and is similar to a sampler previously used for gold tailings (Vermeulen 2001). The upper portion consists of a split solid cylinder with a 1 mm diameter vent hole through its centre; the hole also allowed a 0.75 mm rod to be inserted to confirm that the sampler was full. The sampling tube is 250 mm long, with inner and outer diameters of 75 and 80 mm. The lowest 25 mm of the tube is tapered at 5° to facilitate sampling, and the tube was polished inside and out to minimize friction.

The entire length of the sampling tube was pushed into the tailings from surface level. To minimize disturbance, the sampler was dug out rather than pulled out. It was then opened and the sample marked at 1 cm intervals to obtain 25 slices (Fig S4). A cutting plate was used to slice the sample, and each slice was stored in a labelled, air-tight bag for transport to the laboratory. Slices were numbered 1 to 25 from top to bottom. To achieve a uniform slicing frequency, slices were always cut at 1 cm intervals regardless of the layer boundaries suggested by colour changes. Assuming that colour changes reflect alterations in PSD and mineralogy, some layers could have been thinner than 1 cm. Individual slices are identified by appending the slice number to the sample code. For example, slice *Cyclone UnFl (7)* is the seventh slice from top to bottom of the underflow sample at the Cyclone TSF.

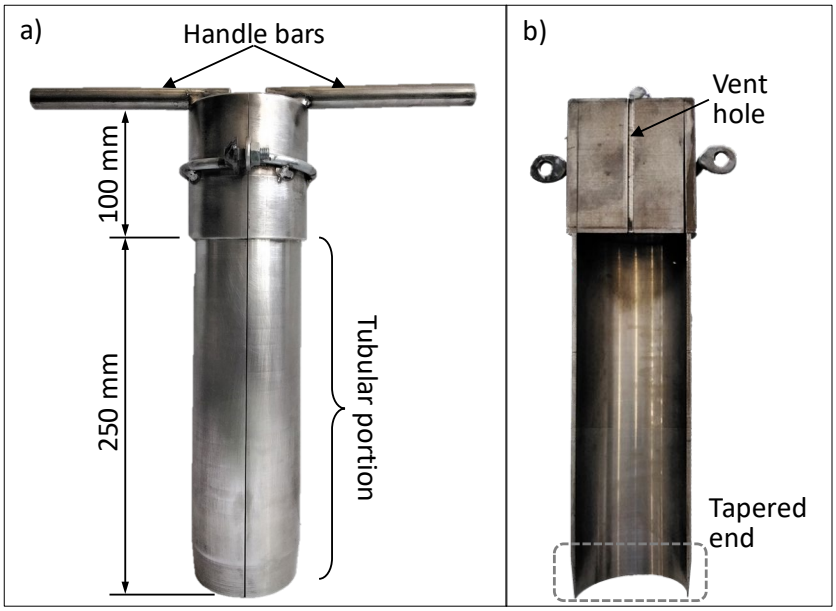

Fig. S3. *Tailings sampler: a) assembled; and b) internal lateral view.*

Fig. S4. *Sample 'Spigot @100' with marks at 1 cm intervals prior to being sliced.*

S2.2 Particle shape and mineralogy

The particle shape of the tailings from the three sampled TSFs was examined by scanning electron microscopy (SEM) on three size fractions isolated by sieving (>150 µm, 75 to 150 µm, and <75 µm). The particles were highly angular regardless of size (Fig S5), as is characteristic of tailings generated by ore crushing.

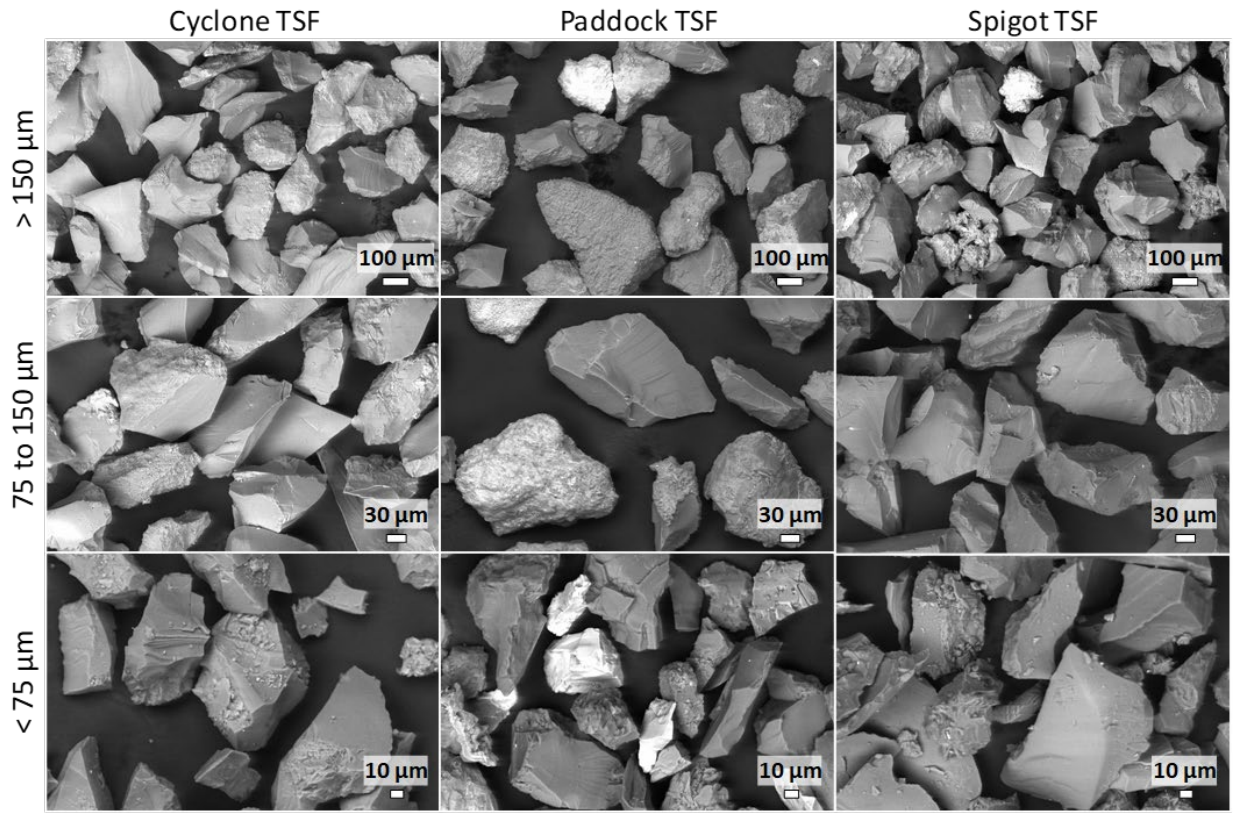

Fig. S5. *Scanning electron microscopy images of the sampled tailings.*

The mineralogy of one slice from each sampled TSF was analysed by X-ray diffraction; each analysed slice had a PSD deemed representative of the respective TSF. Table S1 shows that the tailings from all three TSFs are dominated (>55%) by quartz, in agreement with previous reports for Witwatersrand Basin gold tailings (Chang 2009; Vermeulen 2001). The tailings also contained significant amounts (>8%) of chlorite, and the Paddock TSF contained significant amounts (>8%) of plagioclase, muscovite, and actinolite.

Table S1. Mineralogy of the three sampled TSFs.

Mineral	Cyclone OvFl (2)	Paddock @25 (17)	Spigot @100 (8)
Quartz	77.5	56.4	74.6
Plagioclase	0	8.9	0
Chlorite	8.4	8.5	8.6

Mineral	Cyclone OvFl (2)	Paddock @25 (17)	Spigot @100 (8)
Microcline	0	1.6	0
Muscovite	4.6	8.1	3.2
Pyrophyllite	2.9	4.5	5.8
Talc	0	0	5.3
Hematite	0.6	0	0
Chloritoid	4.0	0	0
Pyrite	0	0	0.7
Dolomite	0	2.9	0
Gypsum	2.0	0	0
Actinolite	0	9.1	0
Calcite	0	0	1.8

Note: *Values are percent by mass. The number in parentheses after each sample code is the slice analysed by X-ray diffraction.*

S2.3 Specific gravity, PSD, and plastic limit

The specific gravity (G_s) was measured following BS 1377:2 (BSI 1990) on the finest and coarsest slice encountered at each TSF. For the Cyclone and Paddock TSFs, G_s was 2.70 and 2.72, respectively, for both slices. For the Spigot TSF, the fine slice yielded 2.59 and the coarsest 2.67. These values are consistent with the quartz-dominated mineralogy (Table S1) and with previously reported G_s values for gold tailings (Chang 2009; Vermeulen 2001).

To assess variability along the length of the samples, the PSD and plastic limit (PL) of each slice were determined. PSDs were measured with a laser diffraction spectroscopy device (Anton Paar PSA 1090) operating over particle sizes from 0.04 to 500 µm. The specimen mass required for each PSD determination ranged between 0.9 and 1.4 g, extracted from the central portion of the top surface of each slice. The dispersing agent was sodium hexametaphosphate (5 g/L) as per ASTM D7928-21 (ASTM 2021). The specimens and dispersing solution were left overnight in the temperature-controlled room housing the device to ensure temperature equilibrium and promote

deflocculation. PL determinations followed the thread-rolling method of BS 1377:2 (BSI 1990). Additional index properties, such as the liquid limit and the minimum and maximum void ratios, were not determined owing to the limited mass of each slice.

Plastic limits could be measured only for a minority of slices; the remainder were non-plastic and could not be rolled into threads. The limited PL results are summarized in Table S2.

Table S2. Plastic limit results.

TSF	Sample	Slice numbers	PL range (%)
Paddock	Paddock @50	1–2	23–27
	Paddock @75	2–4 and 13–20	24–32
	Paddock @100	3–15	24–33
Spigot	Spigot @75	5–7	27–32
	Spigot @100	1–2	30–33

Note: *PL could not be measured for the slices not listed, which were non-plastic. Samples not listed (Cyclone UnFl and OvFl, Paddock @25, Spigot @25 and @50) were non-plastic throughout.*

S3 Profiling at the Remine TSF

Reclamation at the Remine TSF allowed a 3 m deep profile to be exposed for visual appraisal at the location shown in Fig S2d, following an approach similar to that of Vermeulen (2001). Six 0.5 m tall benches were created by cutting into the tailings with the flat blade of a spade, and each vertical face was photographed individually. The resulting profile is presented as Fig 3 in the Note.

S4 Particle size distributions of the individual samples

Figures S6 to S8 show the 25 PSDs measured on each sample collected at the Cyclone, Paddock, and Spigot TSFs. Within every 25 cm sample the curves span a wide range of gradations, illustrating the fine-scale layering discussed in the Note.

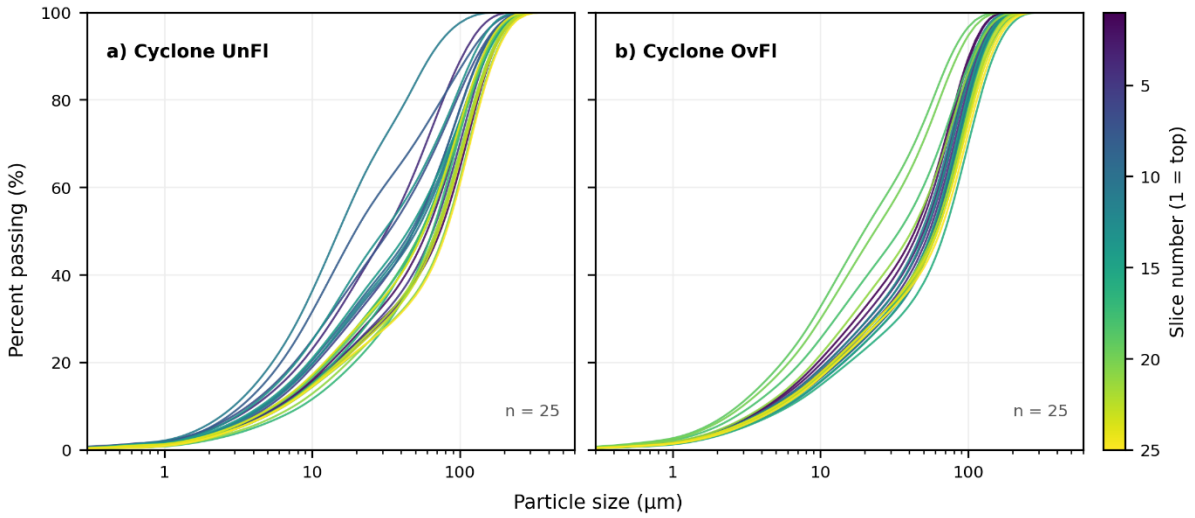

88

89 **Fig. S6.** *Range of PSDs in the samples: a) Cyclone UnFl; and b) Cyclone OvFl.*

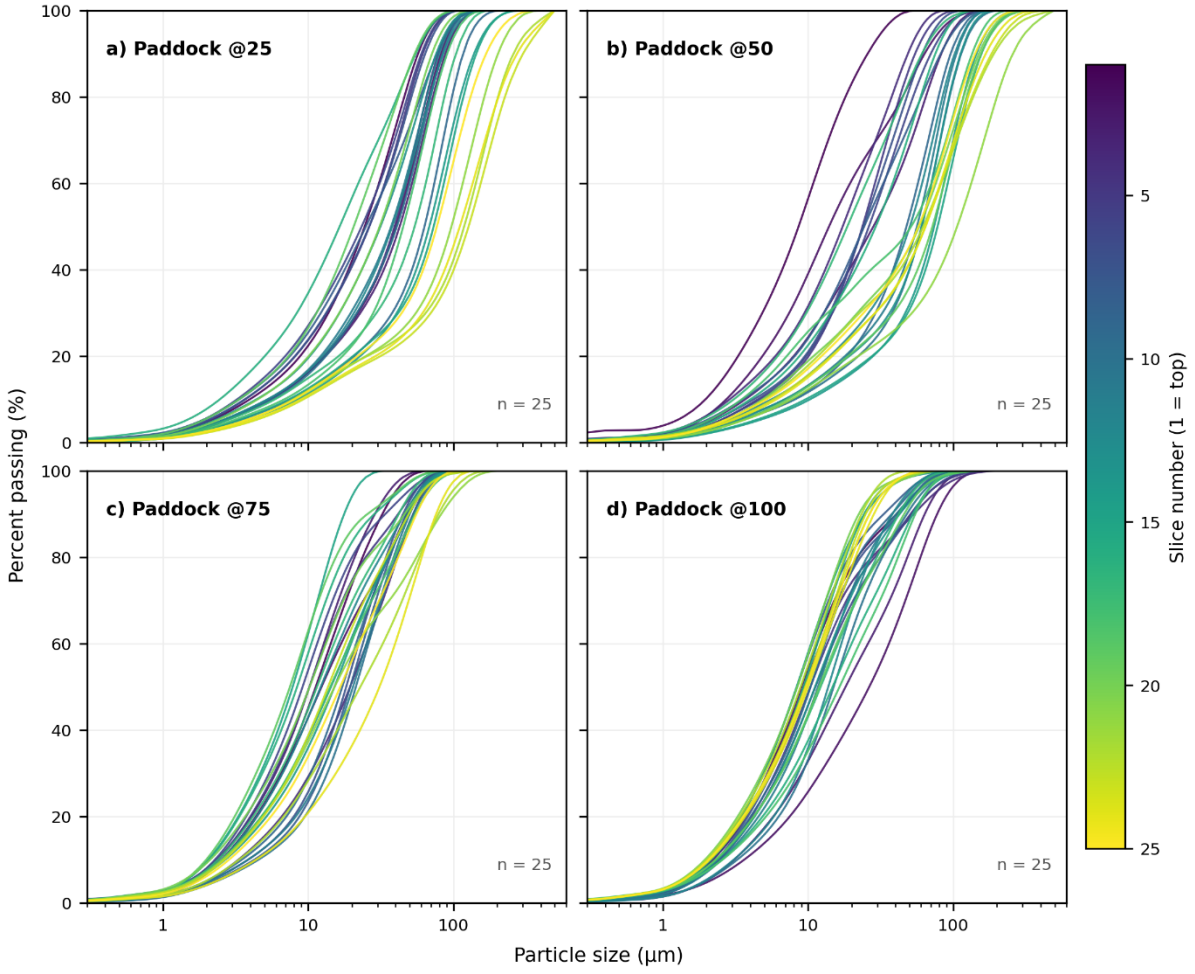

90

Fig. S7. *Range of PSDs in the samples: a) Paddock @25; b) Paddock @50; c) Paddock @75; and d) Paddock @100.*

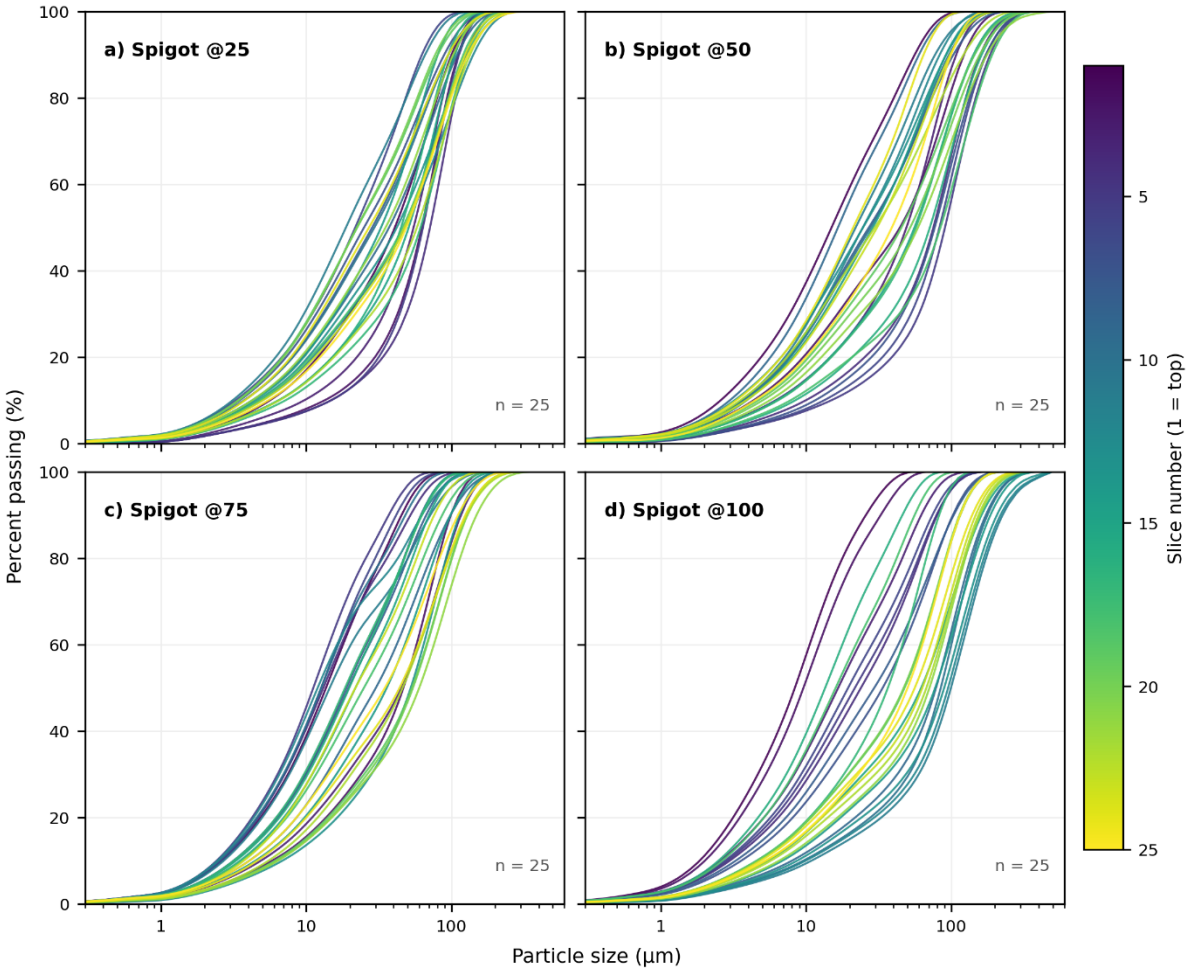

Fig. S8. *Range of PSDs in the samples: a) Spigot @25; b) Spigot @50; c) Spigot @75; and d) Spigot @100.*

S5 D_{50} data for Brumadinho

The 33 Brumadinho D_{50} values plotted in Fig. 2 of the Note were compiled from two sources. Nineteen were digitised from Fig. 4.5 of Pirete da Silva (2010); although that figure's caption refers to 25 PSDs, only 19 D_{50} values could be recovered on digitisation. A further 14 were obtained from the Program 1 and Program 2 sampling campaigns described in Appendix E of Robertson et

al. (2019). All Brumadinho (and Impala) samples correspond to subaerially deposited tailings, consistent with the basis used throughout this study.

REFERENCES

ASTM. (2015). ASTM D1587M-15 Standard practice for thin-walled tube sampling of fine-grained soils for geotechnical purposes.

ASTM. (2021). ASTM D7928-21 Standard test method for particle-size distribution (gradation) of fine-grained soils using the sedimentation (hydrometer) analysis.

BSI. (1990). BS 1377-2 Methods of test for soils for civil engineering purposes — Classification tests.

Chang, H. (2009). The effect of fabric on the behaviour of gold tailings. PhD thesis, University of Pretoria.

McPhail, G., & Wagner, J. (1987). Disposal of residues. In The extractive metallurgy of gold in South Africa.

Pirete da Silva, W. (2010). Study of the static liquefaction potential of an upstream tailings dam applying Olson's (2001) methodology [In Portuguese]. Masters thesis from the Federal University of Ouro Preto, Brazil.

Robertson, P., de Melo, L., Williams, D., & Wilson, G. (2019). Report of the Expert Panel on the Technical Causes of the Failure of Feijão Dam I.

Vermeulen, N. (2001). The composition and state of gold tailings. PhD thesis, University of Pretoria.